Second-Generation of Multiple-Angle Incidence Resolution Spectrometry

*Nobutaka Shioya, Kazutaka Tomita, Takafumi Shimoaka, and Takeshi Hasegawa**

Laboratory of Chemistry for Functionalized Surfaces, Division of Environmental Chemistry, Institute for Chemical Research, Kyoto University, Gokasho, Uji, Kyoto 611-0011, Japan

ABSTRACT. Infrared (IR) surface spectroscopic techniques commonly have long-term issues that 1) the multiple reflections of light in the substrate yield optical interference fringes in the absorption spectrum, and 2) the double-modulation of light at the interferometer in FT-IR makes a water-vapor-subtraction impossible. These measurement troubles often disturb the quantitative analysis of chemical bands of the analyte thin film. Multiple-angle incidence resolution spectrometry (MAIRS) is not an exception on this matter, either. In the present study, the long-term common issues have first been resolved by fixing the angle of incidence at a large angle; whereas the polarization angle is changed. With this simple conceptual change of MAIRS, as a result, we are ready for concentrating on spectral analysis only without concerning about the measurement troubles.

INTRODUCTION

Molecular structural analysis in an organic thin film is gaining importance year by year for strategic design of material functions of a thin-film device used in various kinds of organic electronics represented by photovoltaic devices, light emitting diodes, transistors and chemical sensors. The molecular structure should fully be revealed in terms of the crystallinity and orientation, since both factors in a thin film are often largely different from those of a bulk matter. Unexpectedly, analytical techniques of these key structural factors are still under development. The crystallography for the thin-film analysis is a little ahead to the molecular orientation analysis at the moment. Two-dimensional grazing-incidence X-ray diffraction (2D-GIXD) coupled with a synchrotron radiation source has recently been recognized rapidly as the most powerful technique for the thin-film crystallography.[1-3] Even with the cutting-edge technique, regardless, the diffraction technique works limitedly on crystallized parts only, although polymorph is revealed in detail with a high accuracy.

Molecular orientation analysis on spectroscopy is thus needed, and infrared (IR) spectroscopy is a first choice, since a spectrum provides the orientation information of each chemical group as well as the molecular conformation, packing and the molecular interaction. In recent years, various cutting-edge IR spectroscopic techniques for organic surface species have been proposed,[4-10] which attracts great interests particularly for liquid-crystal polymers and supramolecular materials as well as organic semiconductors. With respect to the molecular orientation analysis in a thin film, multiple-angle incidence resolution spectrometry (MAIRS)[8-11] represented by the p-polarized MAIRS (pMAIRS)[9] technique especially attracts keen attention for the uniquely high analytical accuracy, reproducibility and robustness even for a thin film having a surface roughness, which is not only for theoretical interest, but it is practically useful.[12-17]

MAIRS yields two spectra simultaneously from an identical thin-film sample revealing the in-plane (IP) and out-of-plane (OP) components of each transition moment (Figure 1), which have exactly the same surface selection rules as those of the conventional transmission and reflection-absorption (RA) spectrometry, respectively.[18] Therefore, the two spectra of MAIRS are named as MAIRS-IP and OP spectra. MAIRS is optimized, so that IP and OP spectra would have a common ordinate (absorbance) scale, which is a unique characteristic of MAIRS.[11,19,20] This makes the molecular orientation at each band quite simple: the band intensity ratio of IP to OP spectra ($A_{\mathrm{IP}}/A_{\mathrm{OP}}$) simply yields the orientation angle, α, with a high accuracy.[11,15,20]

$$\alpha = \tan^{-1}\sqrt{\frac{2A_{\mathrm{IP}}}{A_{\mathrm{OP}}}} \qquad (1)$$

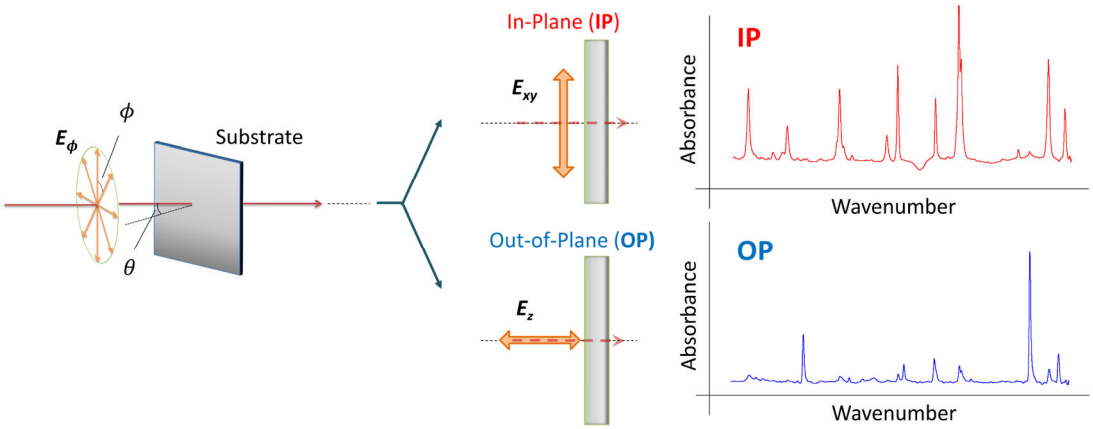

Figure 1. Schematic of the MAIRS2 measurement system. A specific linear polarized ray having an angle of ϕ is irradiated on the film at an angle of incidence of θ. For the measurements, various polarization angles are employed, while the angle of incidence is not changed.

The analytical accuracy of molecular orientation is comparable to that of spectroscopic ellipsometry as long as the sample thickness is less than ca. 500 nm.[15] Another benefit of using

MAIRS is that it requires very few a priori knowledge and assumption for the quantitative orientation analysis,[15,20] as compared to other surface spectroscopic techniques such as vibrational sum frequency generation (SFG)[21] and polarized Raman spectroscopy[22,23]. When MAIRS is coupled with a Fourier transform infrared (FT-IR) spectrometer,[11] an additional benefit is obtained that the polymorph and crystallinity of analytes in a thin film can also be discussed on the accurate band position as related to the molecular orientation.[14,16,17]

Here, we have a big problem that perfect subtraction of the many water-vapor related peaks in the fingerprint region is often difficult,[24-26] and the remained derivative-shaped peaks make key bands of the thin film invisible as shown in Figure 2a. In a similar manner, the interference fringes appear on several substrates such as silicon (Si)[27] and thin-glass plates[28] because of multiple-reflections in the substrate,[29,30] which is further emphasized by the polarizer. Once the fringes appear, even a strong band cannot be analyzed (Figure 3 and Figure S1 in Supporting Information). In the present study, a newly modified MAIRS technique is proposed, which decisively solves both long-term severe problems of "water vapor" and "optical interference fringes" at a time in an ideal manner.

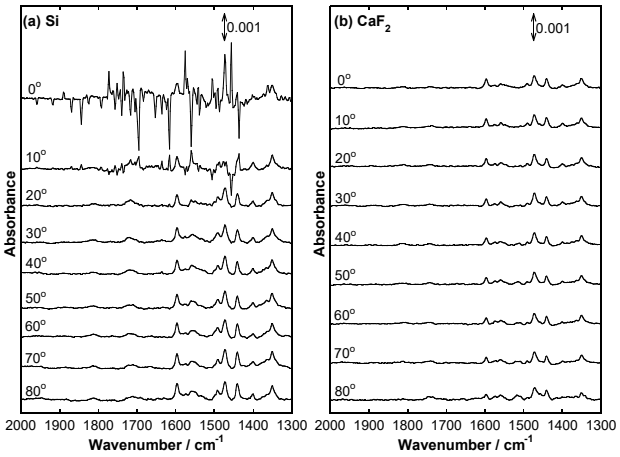

Figure 2. Oblique incidence transmission spectra of tetraphenylporphyrin (H_2TPP) spin-coated thin films deposited on Si (a) and CaF_2 (b) measured using p-polarized light after a water-vapor subtraction.

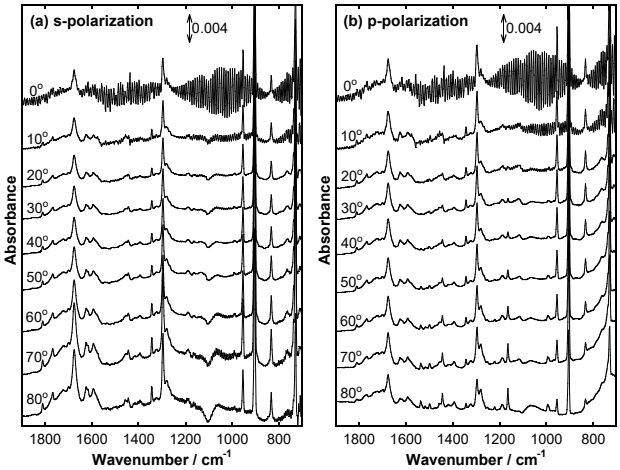

Figure 3. Oblique incidence transmission spectra of pentacene thin films (50 nm) deposited on a Si substrate with a thickness of 0.675 mm for s-polarization (a) and p-polarization (b) after a water-vapor subtraction.

We have a simple question why the water-vapor subtraction is imperfectly done, even after the water-vapor spectrum is carefully prepared by using the same spectrometer. A big hint was

given when the substrate was changed from Si to calcium fluoride (CaF_2). Figure 2 presents some transmission spectra of a thin film deposited on Si and CaF_2 measured at several angles of incidence. The water-vapor related peaks are beautifully removed on CaF_2 (Figure 2b); whereas noisy peaks remain on Si at an angle less than 20° (Figure 2a). We hit on an idea that the reason should be attributed to the reflected light on Si going back to the interferometer, since the reflectance on Si is much higher than that on CaF_2 because of the large difference of the refractive indices of substrate (n_{sub}) in the IR region, i.e., $n_{\mathrm{Si}} = 3.41$ and $n_{\mathrm{CaF_2}} = 1.40$.[31] For the normal incidence, the reflectivity, R, on Si and CaF_2 are simply calculated to be 0.30 and 0.028, respectively, by using the following equation.[9,11] The reflection on CaF_2 can thus be ignored.

$$R = \left|\frac{n_{\mathrm{sub}} - 1}{n_{\mathrm{sub}} + 1}\right|^2 \qquad (2)$$

The reflected light on Si returns to the interferometer to be modulated again, which produces accidental "double modulation." Since the double modulation is out of expectation of FT spectroscopy,[11] this component should yield inaccurate inverse FT calculation giving a slight peak deformation, which would be the reason of the imperfect subtraction.

To prevent the returning of light to the interferometer, the angle of incidence should be made far from nil (at least more than 10°) as found in Figure 2a. The idea of changing the angle close to Brewster's angle of the substrate material, for example, is known to work for eliminating the optical fringes (Figure 3), too.[32,33] Regardless, a small angle less than 10° is needed as long as the conventional MAIRS technique is employed.[19]

Therefore, to make the best use of MAIRS for overcoming the two big matters at once, in the present study, an advanced MAIRS technique named "MAIRS2" is proposed: the angle of

incidence is fixed in a range of 30°–50° to avoid the two problems; whereas the polarization angle is changed instead (Figure 1). Details of the new techniques are described in a later section. As expected, the long-term problems of IR spectroscopy especially for thin film analysis have readily been solved by employing MAIRS2. Since the reproducibility is also quite good, MAIRS2 would be one of the most powerful spectroscopic techniques for thin film analysis.

EXPERIMENTAL SECTION

Sample preparation. Poly(2-perfluorobutyletyl acrylate) (C4FA) was kindly provided by Daikin Industries, Ltd. (Osaka, Japan). A C4FA film was prepared by reference to our previous work.[19] A fluorocarbon-soluble solvent HCFC-225 (a mixture of 225ca and 225cb) was used as the solvent for C4FA, which was purchased from Wako Pure Chemical Industries, Ltd. (Osaka, Japan). The HCFC-225 solution of C4FA at a concentration of 9.56 mg mL^{-1} was spin-coated on a Si substrate at 8000 rpm using an ACTIVE (Saitama, Japan) ACT-300D spin coater. A double-side polished Si wafer having a thickness of 0.675 mm was purchased from Valqua FFT (Tokyo, Japan). The film thickness was determined to be about 50 nm by X-ray reflectivity measurements performed on a Rigaku (Tokyo, Japan) SuperLab X-ray diffractometer.

MAIRS2 measurements. The MAIRS2 technique was constructed on a Thermo Fischer Scientific (Madison, WI) Nicolet iS50 FT-IR spectrometer equipped with a Thermo Fischer Scientific (Yokohama, Japan) automatic MAIRS equipment (TN 10-1500). The FT-modulated IR ray was passed through an angle-controllable wire-grid linear polarizer made of ZnSe incorporated in the spectrometer. The polarization angle was automatically changed from 0° to 90° by 15° steps where the angles of 0° and 90° correspond to the s- and p-polarizations, respectively. The angle of incidence was kept at 45° during the measurements, which is the optimal angle for a Si substrate as discussed later. A mercury cadmium telluride (MCT) detector was employed for detecting the

IR ray. The accumulation number of the single-beam measurements was 256 for each polarization angle. All the measurements were performed under a dry air condition.

RESULTS AND DISCUSSION

Principle of MAIRS2. The new analytical technique, MAIRS2, is constructed as a modification of the original MAIRS theory that is built on a framework using a regression equation as summarized briefly as follows. The IP and OP components of the single-beam spectra are calculated through the classical least square (CLS) regression equation.[11]

$$\boldsymbol{S}_{\mathrm{obs}} = \begin{pmatrix} r_{\mathrm{IP},1} & r_{\mathrm{OP},1} \\ r_{\mathrm{IP},2} & r_{\mathrm{OP},2} \\ \vdots & \vdots \end{pmatrix} \begin{pmatrix} \boldsymbol{S}_{\mathrm{IP}} \\ \boldsymbol{S}_{\mathrm{OP}} \end{pmatrix} + \boldsymbol{U} \equiv \boldsymbol{R} \begin{pmatrix} \boldsymbol{S}_{\mathrm{IP}} \\ \boldsymbol{S}_{\mathrm{OP}} \end{pmatrix} + \boldsymbol{U}$$
$$\begin{pmatrix} \boldsymbol{S}_{\mathrm{IP}} \\ \boldsymbol{S}_{\mathrm{OP}} \end{pmatrix} = (\boldsymbol{R}^{\mathrm{T}}\boldsymbol{R})^{-1}\boldsymbol{R}^{\mathrm{T}}\boldsymbol{S}_{\mathrm{obs}} \qquad (3)$$

Here, $\boldsymbol{S}_{\mathrm{obs}}$ involves a set of single-beam spectra measured at various angles of incidence. These observed spectra are decomposed to have the IP and OP single-beam spectra (denoted as $\boldsymbol{S}_{\mathrm{IP}}$ and $\boldsymbol{S}_{\mathrm{OP}}$, respectively) by using the $\boldsymbol{R}$ matrix depending on only the angle of incidence, θ, where the $\boldsymbol{U}$ matrix contains a non-linear response to $\boldsymbol{R}$. Details of the $\boldsymbol{R}$ and $\boldsymbol{U}$ matrixes are described in the original paper.[10]

As found in eq 3, the intensity of an un-polarized IR-ray at each angle of incidence is a linear combination of the two orthogonal-polarization components, i.e., IP and OP. Here, the s-polarization contributes only to IP in terms of the electric vector irrespective of θ. The p-polarization, on the other hand, contributes to both IP and OP with an intensity ratio of $\sin^2\theta\tan^2\theta + \cos^2\theta : \tan^2\theta$, respectively. As a result, the matrix elements of $\boldsymbol{R}$ at θ_j are

$1 + \sin^2\theta_j \tan^2\theta_j + \cos^2\theta_j$ and $\tan^2\theta_j$.[10] If the polarization dependence of the spectrometer, γ, is taken into account, the $\boldsymbol{R}$ matrix is changed to be:

$$\boldsymbol{R} = \begin{pmatrix} \gamma + \sin^2\theta_1 \tan^2\theta_1 + \cos^2\theta_1 & \tan^2\theta_1 \\ \vdots & \vdots \end{pmatrix} \quad (4)$$

Here, γ is defined as the intensity ratio of the s-polarized light to the p-polarized one at a wavenumber when measured with nothing in the sample room (blank).[18]

$$\gamma \equiv \frac{S^{\mathrm{s}}_{\mathrm{blank}}}{S^{\mathrm{p}}_{\mathrm{blank}}} = \frac{S^{\mathrm{s}}_{\mathrm{BG}}}{S^{\mathrm{p}}_{\mathrm{BG}}} \frac{T^{\mathrm{p}}_{\mathrm{sub}}}{T^{\mathrm{s}}_{\mathrm{sub}}} \quad (5)$$

In practice, however, the background (BG) measurements are performed with a substrate to have $S^{\mathrm{s}}_{\mathrm{BG}}$ and $S^{\mathrm{p}}_{\mathrm{BG}}$. Therefore, the correlation between $S^{\mathrm{s}}_{\mathrm{blank}}$ ($S^{\mathrm{p}}_{\mathrm{blank}}$) and $S^{\mathrm{s}}_{\mathrm{BG}}$ ($S^{\mathrm{p}}_{\mathrm{BG}}$) is needed for convenience. The correlation is simply obtained by using the transmittance of the substrate, T_{sub}, as $S_{\mathrm{BG}} = S_{\mathrm{blank}} T_{\mathrm{sub}}$, which is found in eq 5. Fortunately, T_{sub} can be calculated by using the refractive index of the substrate.[11,18] In this manner, γ is readily obtained from the p- and s-polarized single-beam spectra of the background measurements ($S^{\mathrm{s}}_{\mathrm{BG}}$ and $S^{\mathrm{p}}_{\mathrm{BG}}$, respectively). Note that, as found in Figure S2 (see Supporting Information), γ has a large dispersion, which cannot be ignored.

Now, we are constructing the advanced MAIRS technique (MAIRS2), in which the angle of incidence is fixed at about 45°, and instead the polarization angle is changed. For this purpose, the polarization angle, ϕ_j must be involved in the $\boldsymbol{R}$ matrix in eq 4. The deformation of the matrix is simple that the linear polarization at an angle of ϕ_j is divided into s (0°) and p (90°) polarizations,

whose electric fields have an intensity ratio of $\cos^2\phi_j : \sin^2\phi_j$ (Figure 1). Therefore, eq 4 is re-written as:

$$\boldsymbol{R} = \begin{pmatrix} \gamma\cos^2\phi_1 + \sin^2\phi_1(\sin^2\theta_1 \tan^2\theta_1 + \cos^2\theta_1) & \sin^2\phi_1 \tan^2\theta_1 \\ \vdots & \vdots \end{pmatrix} \tag{6}$$

By introducing eq 6 into eq 3, the MAIRS2-IP and -OP single-beam spectra are obtained from the observed data, and then the corresponding absorbance spectra are readily calculated by using eq 7 where the superscript "sam" stands for "sample."

$$A_{\mathrm{IP}} = -\log\frac{S_{\mathrm{IP}}^{\mathrm{sam}}}{S_{\mathrm{IP}}^{\mathrm{BG}}}, \quad A_{\mathrm{OP}} = -\log\frac{S_{\mathrm{OP}}^{\mathrm{sam}}}{S_{\mathrm{OP}}^{\mathrm{BG}}} \tag{7}$$

Optimization of MAIRS2. MAIRS2 has intrinsically the same principle as found in the conventional MAIRS and pMAIRS. As done for pMAIRS, therefore, the optimal angle of incidence must be determined, so that both IP and OP spectra would have a common absorbance scale.[18,19] In contrast to pMAIRS that is polarization-dependence free, MAIRS2 usually needs an additional correction process[20] as shown below.

Itoh and coworkers reveal physical expressions of MAIRS spectra, which are rigorously deduced from Maxwell's equations.[18] The final results are shown as:

$$\begin{aligned} A_{\mathrm{IP}} &= \frac{8\pi d_2}{\lambda}\left[h_x^{\mathrm{IP}}\,\mathrm{Im}\left(\tilde{\varepsilon}_{\mathrm{r},x}\right) + h_z^{\mathrm{IP}}\,\mathrm{Im}\left(-\frac{1}{\tilde{\varepsilon}_{\mathrm{r},z}}\right)\right] \\ A_{\mathrm{OP}} &= \frac{8\pi d_2}{\lambda}\left[h_x^{\mathrm{OP}}\,\mathrm{Im}\left(\tilde{\varepsilon}_{\mathrm{r},x}\right) + h_z^{\mathrm{OP}}\,\mathrm{Im}\left(-\frac{1}{\tilde{\varepsilon}_{\mathrm{r},z}}\right)\right] \end{aligned} \tag{8}$$

Here, $\mathrm{Im}(\tilde{\varepsilon}_{\mathrm{r},x})$ and $\mathrm{Im}(-1/\tilde{\varepsilon}_{\mathrm{r},z})$ are called transverse and longitudinal optic (TO and LO) energy-loss functions, respectively, which determine the shape of normal-incidence transmission and RA spectra, respectively.[11] The weighting factors, h, are mostly a function of the angle of incidence and the refractive index of substrate. The rest parameters are referred to the reference.[18] If the optimal experimental condition is employed, eqs 8 are simplified to be eqs 9, since $h_z^{\mathrm{IP}} \approx 0$ and $h_x^{\mathrm{OP}} \approx 0$ hold.[18-20]

$$A_{\mathrm{IP}} \approx \frac{8\pi d_2}{\lambda}\left[h_x^{\mathrm{IP}}\,\mathrm{Im}\left(\tilde{\varepsilon}_{\mathrm{r},x}\right)\right]$$
$$A_{\mathrm{OP}} \approx \frac{8\pi d_2}{\lambda}\left[h_z^{\mathrm{OP}}\,\mathrm{Im}\left(-\frac{1}{\tilde{\varepsilon}_{\mathrm{r},z}}\right)\right] \tag{9}$$

These equations apparently indicate that the optimized IP and OP spectra are definitely driven by the TO and LO energy-loss functions, respectively. In short, the optimal angles of incidence should be defined, so that the relations, $h_z^{\mathrm{IP}} \approx 0$ and $h_x^{\mathrm{OP}} \approx 0$, would adequately be satisfied. Here, the weighting factors for MAIRS2 are calculated by using the equations (eq 10) in the paper.[18]

$$h_x^{\mathrm{IP}} = \frac{\sum {Z_{\mathrm{IP}}}'(a^{\mathrm{p}}\sin^2\phi + \varphi\gamma a^{\mathrm{s}}\cos^2\phi)T_{\mathrm{BG}}^{\mathrm{p}}}{\sum {Z_{\mathrm{IP}}}'(\sin^2\phi + \varphi\gamma\cos^2\phi)T_{\mathrm{BG}}^{\mathrm{p}}}$$
$$h_z^{\mathrm{IP}} = \frac{\sum {Z_{\mathrm{IP}}}' b^{\mathrm{p}}\sin^2\phi\, T_{\mathrm{BG}}^{\mathrm{p}}}{\sum {Z_{\mathrm{IP}}}'(\sin^2\phi + \varphi\gamma\cos^2\phi)T_{\mathrm{BG}}^{\mathrm{p}}}$$
$$h_x^{\mathrm{OP}} = \frac{\sum {Z_{\mathrm{OP}}}'(a^{\mathrm{p}}\sin^2\phi + \varphi\gamma a^{\mathrm{s}}\cos^2\phi)T_{\mathrm{BG}}^{\mathrm{p}}}{\sum {Z_{\mathrm{OP}}}'(\sin^2\phi + \varphi\gamma\cos^2\phi)T_{\mathrm{BG}}^{\mathrm{p}}} \tag{10}$$
$$h_z^{\mathrm{OP}} = \frac{\sum {Z_{\mathrm{OP}}}' b^{\mathrm{p}}\sin^2\phi\, T_{\mathrm{BG}}^{\mathrm{p}}}{\sum {Z_{\mathrm{OP}}}'(\sin^2\phi + \varphi\gamma\cos^2\phi)T_{\mathrm{BG}}^{\mathrm{p}}}$$

Details of the parameters in eq 10 are referred to the reference. Calculation of these coefficients readily reveals the optimal angle of incidence for MAIRS2. The optimal angles for representative IR-transparent materials are uniquely determined by finding $h_z^{\mathrm{IP}} \approx 0$ and $h_x^{\mathrm{OP}} \approx 0$, which are summarized in Table 1. For example, the optimal angle for Si is found to be 45° (see Figure S3). Of another note is that the polarizing angle is nearly independent of the weighting factor as found by a similar calculation (data not shown).

Table 1. The optimal angle of incidence and the substrate-specific parameter of various IR-transparent materials calculated for MAIRS2 analysis.

Material	Refractive index[31]	Optimal angle of incidence	Substrate specific parameter, H
Germanium (Ge)	4.00	45	0.33
Silicon (Si)	3.41	45	0.33
Diamond (C)	2.41	44	0.34
Zinc selenide (ZnSe)	2.40	44	0.34
KRS-5 ($TlBr_{0.42}I_{0.58}$)	2.37	44	0.34
Zinc sulfide (ZnS)	2.25	43	0.35
Silver chloride (AgCl)	1.90	41	0.38
Cesium iodine (CsI)	1.73	39	0.41
Potassium bromide (KBr)	1.52	35	0.49
Sodium chloride (NaCl)	1.49	35	0.49
Quartz (SiO_2)	1.47	34	0.51
Barium fluoride (BaF_2)	1.45	34	0.51
Potassium chloride (KCl)	1.45	34	0.51
Calcium fluoride (CaF_2)	1.40	33	0.53
Lithium fluoride (LiF)	1.39	32	0.55

Next, a substrate-specific parameter, $H \equiv h_x^{\mathrm{IP}}/h_z^{\mathrm{OP}}$, is calculated, which is the key of the intensity scaling of the OP spectrum, since the scaling factor is obtained as n^4H (n; refractive

index of the film) as mentioned elsewhere.[20] The calculated values are listed in Table 1 together with the optimal angle of incidence. In this manner, the optimization has been done.

Note that a MAIRS2-IP spectrum corresponds to an s-polarized transmission spectrum, whose intensity is influenced by the angle of incidence,[11,18] since the angle is fixed for MAIRS2. To make the IP spectrum quantitatively meet with the normal-incidence transmission spectrum ($\theta = 0°$), therefore, the intensity (absorbance) correction is needed. The correction is easily done by calculating the intensity ratio of the s-polarized transmission spectra, $a_s^{\theta=0°}/a_s^{\theta}$, since the coefficient of the IP spectrum nearly equals to a_s^{θ}, which is theorized rigorously.[18] The calculated values are referred to Table S1.

Now, we are ready for optimizing the MAIRS2 spectra. The optimal spectra are represented by:

$$A_{\mathrm{IP}}{}' = \frac{a_s^{\theta=0°}}{a_s^{\theta}} A_{\mathrm{IP}}$$
$$A_{\mathrm{OP}}{}' = \frac{a_s^{\theta=0°}}{a_s^{\theta}} n^4 H A_{\mathrm{OP}} \qquad (11)$$

For the correction of the intensity scale of the OP spectra, not only the normalized factor, but also an additional factor of n^4H is needed as found in pMAIRS.[20]

Performance of MAIRS2. The quality of MAIRS2 spectra is checked by using a standard sample of a perfluorinated polymer (C4FA) thin layer as shown in Figure 4a. The raw single-beam spectra before the MAIRS calculation are available in Figure S4 for reference. The C4FA layer is the same as used for checking pMAIRS spectra,[18] which plays a role to exhibit an apparent band splitting of the CF_2 stretching vibration mode between the IP and OP spectra reflecting the TO-

LO splitting.[11,34,35] In fact, the splitting is found at about 1135 cm^{-1}, and the OP band appears at higher wavenumber than the IP one. When these MAIRS2 spectra are compared to pMAIRS spectra (Figure 4b), the band position, absolute intensity and shape of the MAIRS2 spectra are nearly identical to those of pMAIRS.[19] In this manner, the correction using eqs 6~11 is found to work very well.

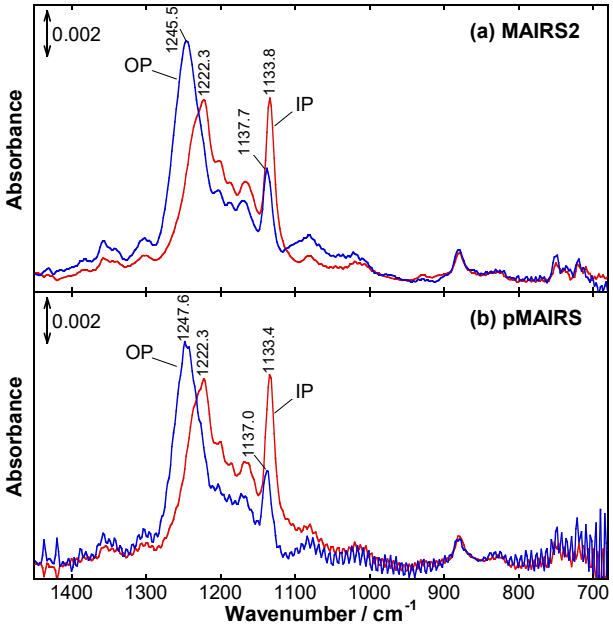

Figure 4. Optimized MAIRS2 (a) and pMAIRS (b) spectra of a C4FA (n = 1.35) spin-coated thin film deposited on a Si substrate. The red and blue lines are the IP and OP spectra, respectively.

One of the most significant impacts using MAIRS2 is an effective removal of interference fringes. Figure 4b presents pMAIRS spectra having interference fringes seriously. Optical interference fringes are caused by multiple reflections in a coincidental thickness combination of the substrate and film especially for the normal incidence. Apparent fringes are over laid on the spectra over a wide wavenumber region, particularly for the OP spectrum in Figure 4b. As a result,

an accurate peak position of C4FA is impossible to find, which is greatly resolved by using MAIRS2 as found in Figure 4a.

Another advantage of using MAIRS2 is that the water-vapor peaks are successfully subtracted by rejecting the problem of double modulation. Figure 5 presents MAIRS2 and pMAIRS spectra of a tetraphenylporphyrin (H_2TPP) thin film after the subtraction of a water-vapor spectrum. Since a thin film of an organic semiconductor typically has a very weak absorbance in the water-vapor region,[16,17] the imperfect subtraction issue becomes a serious problem especially in humid conditions. The pMAIRS spectra, in fact, have noisy water-vapor peaks with positive and negative signs in the region of 1800–1400 cm^{-1} as found in Figure 5b. If the imperfect subtraction is truly attributed to the spectral deformation due to the 'double modulation,' MAIRS2 is expected to resolve this matter. The MAIRS2 spectra of the same sample, as expected, have overcome the water-peaks matter, and the absorption bands of H_2TPP are indeed recognized in the fingerprint region (Figure 5a).

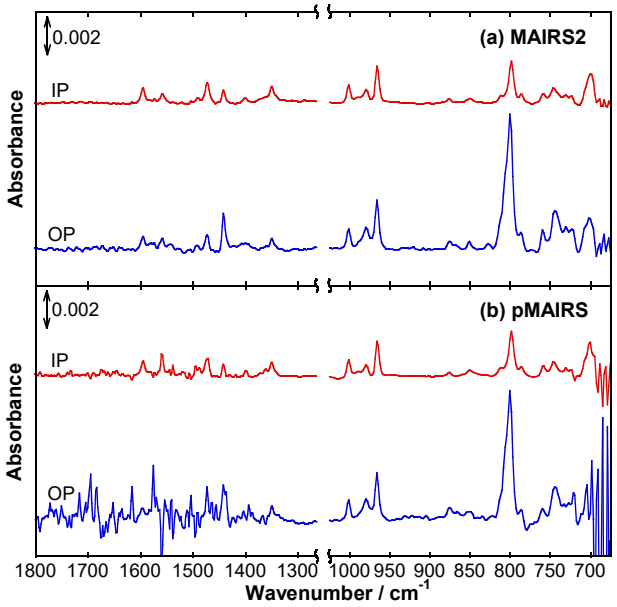

Figure 5. Optimized MAIRS2 (a) and pMAIRS (b) spectra of an H_2TPP (n = 1.62) spin-coated thin film deposited on a Si substrate. The red and blue lines are the IP and OP spectra, respectively.

Of another note is that the MAIRS2 spectra detect the band of H_2TPP at about 700 cm^{-1} (Figure 5a); whereas artifact noise overlaps with the sample peaks in the pMAIRS one (Figure 5b). This characteristic becomes important when a compound having aromatic rings such as H_2TPP is analyzed, since the orientation-sensitive band of the C–H out-of-plane deformation vibration mode appears typically in this wavenumber region.[13,14,16,17]

In addition, the conventional MAIRS techniques intrinsically have a problem that the light-irradiating area on the sample changes when the angle of incidence is changed, which induces a concern that different portions of light attain the detector. To prevent this concern, the aperture (J-stop) is fully opened during the MAIRS measurements.[36] Since MAIRS2 employs a fixed angle of incidence referring to Table 1, this concern is resolved.

CONCLUSION

We have developed an advanced MAIRS technique for obtaining infrared spectra of a thin film free from interference fringes. This new technique is constructed based on a simple idea that the polarization angle is used as a measurement variable for extracting the IP and OP spectra, while the angle of incidence is kept at ~45°. When comparing to the conventional MAIRS technique using various angles of incidence including a small angle less than 10°, avoiding the small angle provides many significant advantages as follows:

1) The problem of double-modulation is overcome, and as a result water-vapor peaks are subtracted almost ideally.
2) Interference fringes due to the multiple reflections in the substrate never appear no matter what substrate is chosen.
3) Light irradiating area on the sample is fixed.
4) Selection of the aperture size and detector is not limited.

In this manner, MAIRS2 realizes highly robust measurements as compared to the conventional MAIRS techniques. Therefore, MAIRS2 is an alternative powerful spectroscopic tool for the structural characterization in functionalized ultrathin films.

ASSOCIATED CONTENT

Supporting Information.

The following files are available free of charge.

Oblique incidence transmission spectra in a high wavenumber region, Normalized coefficients of MAIRS2, polarizer dependence, and observed single-beam spectra (PDF)

AUTHOR INFORMATION

Corresponding Author

*E-mail: htakeshi@scl.kyoto-u.ac.jp

Author Contributions

The manuscript was written through contributions of all authors.

ORCID

Takeshi Hasegawa: 0000-0001-5574-9869

Notes

The authors declare no competing financial interest.

ACKNOWLEDGMENTS

This work was financially supported by a Grant-in-Aid for Scientific Research (A) (No. 15H02185 (TH)), Grant-in-Aid for Young Scientists (B) (No. 17K14502 (TS)) and Grant-in-Aid for Young Scientists (No. 19K15602 (NS)) from the Japan Society for the Promotion of Science (JSPS), to which the authors' thanks are due.

REFERENCES

1. Rivnay, J.; Mannsfeld, S. C.; Miller, C. E.; Salleo, A.; Toney, M. F. Quantitative Determination of Organic Semiconductor Microstructure from the Molecular to Device Scale. *Chem. Rev.* **2012**, *112*, 5488–5519.

2. DeLongchamp, D. M.; Kline, R. J.; Fischer, D. A.; Richter, L. J.; Toney, M. F. Molecular Characterization of Organic Electronic Films. *Adv. Mater.* **2011**, *23*, 319–337.

3. Chabinyc, M. L. X-ray Scattering from Films of Semiconducting Polymers. *Polym. Rev.* **2008**, *48*, 463–492.

4. Hinrichs, K.; Shaykhutdinov, T. Polarization-Dependent Atomic Force Microscopy–Infrared Spectroscopy (AFM-IR): Infrared Nanopolarimetric Analysis of Structure and Anisotropy of Thin Films and Surfaces. *Appl. Spectrosc.* **2018**, *72*, 817–832.

5. Anton, A.; Steyrleuthner, R.; Kossack, W.; Neher, D.; Kremer, F. Infrared Transition Moment Orientational Analysis on the Structural Organization of the Distinct Molecular Subunits in Thin Layers of a High Mobility n‐Type Copolymer. *J. Am. Chem. Soc.* **2015**, *137*, 6034–6043.

6. Westermeier, C.; Cernescu, A.; Amarie, S.; Liewald, C.; Keilmann, F.; Nickel, B. Sub-Micron Phase Coexistence in Small-Molecule Organic Thin Films Revealed by Infrared Nano-Imaging. *Nat. Commun.* **2014**, *5*, 4101.

7. Liu, H.-B.; Venkataraman, N. V.; Bauert, T. E.; Textor, M.; Xiao, S.-J. Multiple Transmission−Reflection Infrared Spectroscopy for High-Sensitivity Measurement of Molecular Monolayers on Silicon Surfaces. *J. Phys. Chem. A* **2008**, *112*, 12372–12377.

8. Hasegawa, T. A New Approach to Analysis of Molecular Structure in Thin Films: Infrared Multiple-Angle Incidence Resolution Spectrometry. *Appl. Spectrosc. Rev.* **2008**, *43*, 181–201.

9. Hasegawa, T. Advanced Multiple-Angle Incidence Resolution Spectrometry for Thin-Layer Analysis on a Low-Refractive-Index Substrate. *Anal. Chem.* **2007**, *79*, 4385–4389.

10. Hasegawa, T. A Novel Measurement Technique of Pure Out-of-Plane Vibrational Modes in Thin Films on a Nonmetallic Material with No Polarizer. *J. Phys. Chem. B* **2002**, *106*, 4112–4115.

11. Hasegawa, T. Quantitative Infrared Spectroscopy for Understanding of a Condensed Matter; Springer Japan: Tokyo, 2017.

12. Wang, C.; Hosomi, T.; Nagashima, K.; Takahashi, T.; Zhang, G.; Kanai, M.; Zeng, H.; Mizukami, W.; Shioya, N.; Shimoaka, T. et al. Rational Method of Monitoring Molecular Transformations on Metal Oxide Nanowire Surfaces. *Nano Lett.* **2019**, *19*, 2443–2449.

13. Nakamura, T.; Shioya, N.; Shimoaka, T.; Nishikubo, R.; Hasegawa, T.; Saeki, A.; Murata, Y.; Murdey, R.; Wakamiya, A. Molecular Orientation Change in Naphthalene Diimide Thin Films Induced by Removal of Thermally Cleavable Substituents. *Chem. Mater.* **2019**, *31*, 1729–1737.

14. Shioya, N.; Murdey, R.; Nakao, K.; Yoshida, H.; Koganezawa, T.; Eda, K.; Shimoaka, T.; Hasegawa, T. Alternative Face-on Thin Film Structure of Pentacene. *Sci. Rep.* **2019**, *9*, 579.

15. Ishige, R.; Tanaka, K.; Ando, S. In Situ Analysis of Chain Orientation Behavior in Thin Film Aromatic Polyimides by Variable Temperature pMAIRS during Thermal Imidization. *Macromol. Chem. Physi.* **2018**, *219*, 1700370.

16. Shioya, N.; Shimoaka, T.; Eda, K.; Hasegawa, T. Controlling Mechanism of Molecular Orientation of Poly(3-alkylthiophene) in a Thin Film Revealed by Using pMAIRS. *Macromolecules* **2017**, *50*, 5090–5097.

17. Hada, M.; Shioya, N.; Shimoaka, T.; Eda, K.; Hada, M.; Hasegawa, T. Comprehensive Understanding of Structure-Controlling Factors of a Zinc Tetraphenylporphyrin Thin Film Using pMAIRS and GIXD Techniques. *Chem. Eur. J.* **2016**, *22*, 16539–16546.

18. Itoh, Y.; Kasuya, A.; Hasegawa, T. Analytical Understanding of Multiple-Angle Incidence Resolution Spectrometry Based on a Classical Electromagnetic Theory. *J. Phys. Chem. A* **2009**, *113*, 7810–7817.

19. Shioya, N.; Norimoto, S.; Izumi, N.; Hada, M.; Shimoaka, T.; Hasegawa, T. Optimal Experimental Condition of IR pMAIRS Calibrated by Using an Optically Isotropic Thin Film Exhibiting the Berreman Effect. *Appl. Spectrosc.* **2017**, *71*, 901–910.

20. Shioya, N.; Shimoaka, T.; Murdey, R.; Hasegawa, T. Accurate Molecular Orientation Analysis Using Infrared p-Polarized Multiple-Angle Incidence Resolution Spectrometry (pMAIRS) Considering the Refractive Index of the Thin Film Sample. *Appl. Spectrosc.* **2017**, *71*, 1242–1248.

21. Bhattacharyya, D.; Montenegro, A.; Dhar, P.; Mammetkuliyev, M.; Pankow, R. M.; Jung, M. C.; Thompson, M. E.; Thompson, B. C.; Benderskii, A. V. Molecular Orientation of Poly-3-

hexylthiophene at the Buried Interface with Fullerene. *J. Phys. Chem. Lett.* **2019**, *10*, 1757–1762.

22. Wood, S.; Rigas, G.-P.; Zoladek-Lemanczyk, A.; Blakesley, J. C.; Georgakopoulos, S.; Mas-Torrent, M.; Shkunov, M.; Castro, F. A. Precise Characterisation of Molecular Orientation in a Single Crystal Field-Effect Transistor Using Polarised Raman Spectroscopy. *Sci. Rep.* **2016**, *6*, 33057.

23. Itoh, Y.; Hasegawa, T. Polarization Dependence of Raman Scattering from a Thin Film Involving Optical Anisotropy Theorized for Molecular Orientation Analysis. *J. Phys. Chem. A* **2012**, *116*, 5560–5570.

24. Perez-Guaita, D.; Kuligowski, J.; Quintás, G.; Garrigues, S.; de la Guardia, M. Atmospheric Compensation in Fourier Transform Infrared (FT-IR) Spectra of Clinical Samples. *Appl. Spectrosc.* **2013**, *67*, 1339–1342.

25. Chen, Y.; Wang, H.-S.; Umemura, J. A New Method to Obtain Fourier Transform Infrared Spectra Free from Water Vapor Disturbance. *Appl. Spectrosc.* **2010**, *64*, 1186–1189.

26. Bruun, S.; Kohler, A.; Adt, I.; Sockalingum; Manfait, M.; Martens, H. Correcting Attenuated Total Reflection–Fourier Transform Infrared Spectra for Water Vapor and Carbon Dioxide. *Appl. Spectrosc.* **2006**, *60*, 1029–1039.

27. Shioya, N.; Shimoaka, T.; Hasegawa, T. Fringe and Noise Reductions of pMAIRS Spectra Using Principal Component Analysis. *Anal. Sci.* **2017**, *33*, 117–120.

28. Hasegawa, T.; Nakano, Y.; Ishii, Y. Molecular Orientation Analysis of a Single-Monolayer Langmuir-Blodgett Film on a Thin Glass Plate by Infrared Multiple-Angle Incidence Resolution Spectrometry. *Anal. Chem.* **2006**, *78*, 1739–1742.

29. Gunde, M. Optical Effects in IR Spectroscopy: Thickness-Dependent Positions of Absorbance Lines in Spectra of Thin Films. *Appl. Spectrosc.* **1992**, *46*, 365–372.

30. Yamamoto, K; Ishida, H. Interpretation of Reflection and Transmission Spectra for Thin Films: Transmission. *Appl. Optics* **1995**, *34*, 4177–4185.

31. Tasumi, M.; Sakamoto, A. *Introduction to Experimental Infrared Spectroscopy*; John Wiley: Chichester, 2015; p 16.

32. Harrick, N. Transmission Spectra without Interference Fringes. *Appl. Spectrosc.* **1977**, *31*, 548–549.

33. Carson, G.; Granick, S. Infrared Spectra of Organic Monolayers on Mica. *Appl. Spectrosc.* **1989**, *43*, 473–476.

34. Berreman, D. W. Infrared Absorption at Longitudinal Optic Frequency in Cubic Crystal Films. *Phys. Rev.* **1963**, *130*, 2193–2198.

35. Yamamoto, K; Masui, A. TO-LO Splitting in Infrared Spectra of Thin Films. *Appl. Spectrosc.* **1996**, *50*, 759–763.

36. Hasegawa, T.; Matsumoto, L.; Kitamura, S.; Amino, S.; Katada, S.; Nishijo, J. Optimum Condition of Fourier Transform Infrared Multiple-Angle Incidence Resolution Spectrometry for Surface Analysis. *Anal. Chem.* **2002**, *74*, 6049–6054.

TOC Graphic

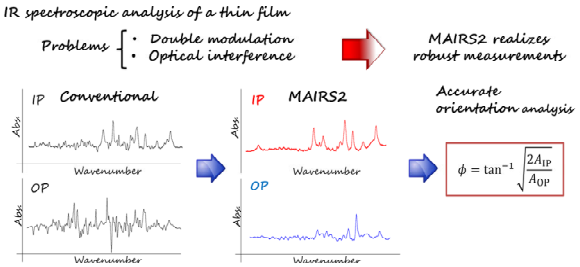
IR spectroscopic analysis of a thin film
Problems
Double modulation
Optical interference
MAIRS2 realizes robust measurements
IP
Conventional
OP
Abs.
Wavenumber
IP
MAIRS2
OP
Accurate orientation analysis
$\phi = \tan^{-1}\sqrt{\frac{2A_{IP}}{A_{OP}}}$